Critical-Point Symmetry in a Finite System

A. Leviatan[1] and J. N. Ginocchio[2]

[1]*Racah Institute of Physics, The Hebrew University, Jerusalem 91904, Israel*

[2]*Theoretical Division, Los Alamos National Laboratory, Los Alamos, New Mexico, 87545, USA*

(Received 12 March 2003; published 29 May 2003)

At a critical point of a second-order phase transition the intrinsic energy surface is flat and there is no stable minimum value of the deformation. However, for a finite system, we show that there is an effective deformation which can describe the dynamics at the critical point. This effective deformation is determined by minimizing the energy surface after projection onto the appropriate symmetries. We derive analytic expressions for energies and quadrupole rates which provide good estimates for these observables at the critical point.

DOI: 10.1103/PhysRevLett.90.212501 PACS numbers: 21.60.Fw, 05.70.Jk, 21.10.Re

Dynamical systems such as nuclei can undergo phase transitions associated with a change of shape of their equilibrium configuration. It has been recognized recently [1,2] that it is possible to formulate the concept of a dynamical symmetry (here meaning solvability in terms of quantum numbers) for systems at the critical point of such shape phase transitions. The importance of these critical-point symmetries lies in the fact that they provide a classification of states and analytic expressions for observables in regions where the structure changes most rapidly. For nuclei, two critical-point symmetries, called E(5) [1] (not the Euclidean group in five dimensions) and X(5) [2], were considered in the geometric framework of the collective model. This model involves a Bohr Hamiltonian which describes the dynamics of a macroscopic quadrupole shape via a differential equation in the intrinsic quadrupole shape variables β and γ. The E(5) [X(5)] critical-point symmetry (CPS) is applicable to a second- [first-] order shape phase transition between spherical and deformed γ-unstable [axially symmetric] nuclei. In the present work we focus on the E(5) CPS for which an empirical example has been found in ^{134}Ba [3,4] and possibly in ^{104}Ru [5], ^{102}Pd [6], and ^{108}Pd [7]. To apply the E(5) CPS to real nuclei one has to take into account the finite number of nucleons. This can be conveniently done in the algebraic framework of the interacting boson model (IBM) [8]. This model describes low-lying quadrupole collective states in nuclei in terms of a system of N monopole (s) and quadrupole (d) bosons representing valence nucleon pairs. The IBM Hamiltonian relevant to the critical point of the phase transition between spherical and γ-unstable deformed nuclei preserves the O(5) symmetry [9]. Its energy surface, obtained by the method of coherent states [9,10], is γ independent and exhibits a flat-bottomed behavior in β which resembles the infinite square-well potential used to derive the E(5) CPS in the geometric approach [1]. Calculations with finite N values ($N = 5$ for ^{134}Ba) have found that this critical IBM Hamiltonian can replicate numerically the E(5) CPS and its analytic predictions [3,5–7]. In the present work we examine the properties and conditions that enable features of E(5) CPS to occur in a finite system. For that purpose we propose wave functions of a particular analytic form, which can simulate accurately the exact IBM eigenstates at the critical point. These wave functions with fixed N and good O(5) symmetry are used to derive accurate estimates for energies and quadrupole rates at the critical point without invoking large-N approximations. The proposed wave functions can be obtained by projection from intrinsic states with an effective β deformation.

In the geometric approach the E(5) eigenfunctions [1] are proportional to Bessel functions of order $\tau + \frac{3}{2}$ and the corresponding eigenvalues are proportional to $(x_{\xi,\tau})^2$. Here τ is the O(5) quantum number, and $x_{\xi,\tau}$ is the ξth root of these Bessel functions. A portion of an E(5)-like spectrum is shown in Fig. 1. It consists of states, $L^+_{\xi,\tau}$, arranged in major families labeled by $\xi = 1, 2, \ldots$ and O(5) τ multiplets ($\tau = 0, 1, \ldots$) within each family. The

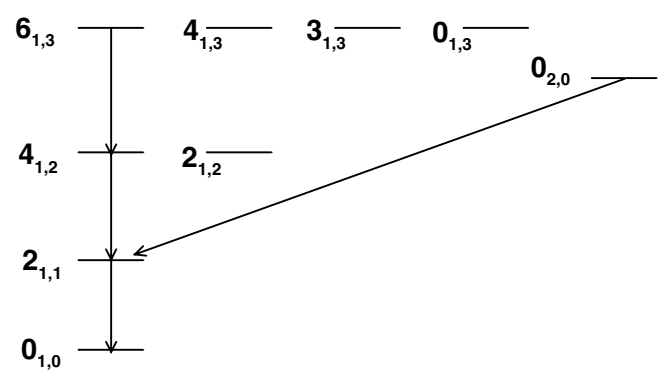

FIG. 1. An E(5)-like spectrum of states labeled by $L_{\xi,\tau}$. Shown are the transitions whose $B(E2)$ values are given in Eq. (9). The $E2$ rates for other $\Delta\tau = 1$ transitions (not shown) are governed by O(5) symmetry. Specifically, $B(E2; L^+_{1,2} \to 2^+_{1,1})$ for $L = 4, 2$ are in the ratio 1:1, respectively, $B(E2; L^+_{1,3} \to 4^+_{1,2})$ for $L = 6, 4, 3$ and $B(E2; L^+_{1,3} \to 2^+_{1,2})$ for $L = 4, 3, 0$ are in the ratios 1:10/21:2/7:11/21:5/7:1, respectively.

 © 2003 The American Physical Society

angular momenta L for each τ multiplet are obtained by the usual O(5) $\supset$ O(3) reduction [11]. The E(5) CPS leads to analytic parameter-free predictions for energy ratios and $B(E2)$ ratios that persist when carried over to a finite-depth potential [12]. As seen in Table I, the E(5) predicted values are in between the values expected of a spherical vibrator [U(5)] and a deformed γ-unstable rotor [O(6)].

In the algebraic approach, the U(5)-O(6) transition region is modeled by the Hamiltonian

$$H = \epsilon \hat{n}_d + \tfrac{1}{4}A[d^\dagger \cdot d^\dagger - (s^\dagger)^2][\text{H.c.}], \tag{1}$$

where ϵ and A are positive parameters. Here $\hat{n}_d$ is the d-boson number operator, H.c. stands for Hermitian conjugate, and the dot implies a scalar product. In the U(5) limit ($A = 0$), the spectrum of H is harmonic, ϵn_d, with $n_d = 0, 1, 2, \ldots, N$. The eigenstates are classified according to the chain U(6) $\supset$ U(5) $\supset$ O(5) $\supset$ O(3) with quantum numbers $|N, n_d, \tau, L\rangle$ (for $\tau \geq 6$ an additional multiplicity index is required for complete classification). These states can be organized into sets characterized by $n_d = \tau + 2k$. States in the lowest-energy set ($k = 0$) satisfy $P_0|N, n_d = \tau, \tau, L\rangle = 0$ with $P_0^\dagger = d^\dagger \cdot d^\dagger$. Other sets ($k > 0$) are generated by $|N, n_d, \tau, L\rangle \propto (P_0^\dagger)^k|N - 2k, n_d = \tau, \tau, L\rangle$. In the O(6) limit ($\epsilon = 0$), the spectrum is $\frac{1}{4}A(N - \sigma)(N + \sigma + 4)$ with $\sigma = N, N - 2, N - 4, \ldots, 0$ or 1. The eigenstates are classified according to the chain U(6) $\supset$ O(6) $\supset$ O(5) $\supset$ O(3) with quantum numbers $|N, \sigma, \tau, L\rangle$. The ground band has $\sigma = N$ and its members satisfy $P_1|N, \sigma = N, \tau, L\rangle = 0$ with $P_1^\dagger = [d^\dagger \cdot d^\dagger - (s^\dagger)^2]$. The remaining bands with $\sigma = N - 2k$ are generated by $|N, \sigma, \tau, L\rangle \propto (P_1^\dagger)^k|N - 2k, \sigma, \tau, L\rangle$. These results suggest that in between the U(5) and O(6) limits, we consider a ground band ($\xi = 1$) for the Hamiltonian (1) determined by the condition

$$P_y|\xi = 1; y, N, \tau, L\rangle = 0, \qquad P_y^\dagger = [d^\dagger \cdot d^\dagger - y(s^\dagger)^2]. \tag{2}$$

In the U(5) basis these states are

$$|\xi = 1; y, N, \tau, L\rangle = \sum_{n_d} \frac{1}{2}[1 + (-1)^{n_d - \tau}]\xi_{n_d,\tau}|N, n_d, \tau, L\rangle, \tag{3}$$

and the n_d summation covers the range $\tau \leq n_d \leq N$. The coefficients $\xi_{n_d,\tau}$ have the explicit form

$$\begin{aligned} \xi_{n_d,\tau} &= \left[\frac{(N - \tau)!(2\tau + 3)!!}{(N - n_d)!(n_d - \tau)!!(n_d + \tau + 3)!!}\right]^{1/2} \times y^{(n_d - \tau)/2}\xi_{\tau,\tau}, \\ (\xi_{\tau,\tau})^2 &= \frac{2(N - \tau + 1)}{(2\tau + 3)!!} y^{2\tau+3}[G_{N+1-\tau}^{(\tau+1)}(y)]^{-1}, \\ G_\alpha^{(n)}(y) &= 2y^{2n+1}\sum_p \binom{\alpha}{2p + 1} y^{2p} \frac{(2p + 1)!!}{(2p + 2n + 1)!!}. \end{aligned} \tag{4}$$

Members of the first excited band ($\xi = 2$) have approximate wave functions of the form

$$\begin{aligned} |\xi = 2; y, N, \tau, L\rangle &= \mathcal{N}_\beta P_y^\dagger|\xi = 1; y, N - 2, \tau, L\rangle, \\ \mathcal{N}_\beta &= [2(2N + y^2 + 1) + 4(y^2 - 1)S_{1,\tau}^{(N-2)}]^{-1/2}, \end{aligned} \tag{5}$$

where $S_{1,\tau}^{(N)}$ is defined in Eq. (7) below.

The states of Eqs. (3) and (5) have fixed N, L, and good O(5) symmetry τ. Henceforth, for reasons to be explained below, they are referred to as τ-projected states. Diagonal matrix elements of the Hamiltonian (1) in these states, denoted by $E_{\xi,\tau} = \langle \xi; y, N, \tau|H|\xi; y, N, \tau\rangle$, can be evaluated in closed form

$$\begin{aligned} E_{\xi=1,\tau} &= \epsilon[N - S_{1,\tau}^{(N)}] + \tfrac{1}{4}A(1 - y)^2 S_{2,\tau}^{(N)}, \\ E_{\xi=2,\tau} &= \epsilon\{N - 2\mathcal{N}_\beta^2[2y^2 + (2N + 7y^2 - 1)S_{1,\tau}^{(N-2)} + 2(y^2 - 1)S_{2,\tau}^{(N-2)}]\} \\ &\quad + \tfrac{1}{4}A2\mathcal{N}_\beta^2\{2(y - 1)^2(y^2 - 1)S_{3,\tau}^{(N-2)} + (y - 1)^2(2N + y^2 - 8y + 5)S_{2,\tau}^{(N-2)} + 16(y - 1)(N + y)S_{1,\tau}^{(N-2)} \\ &\quad + 2[(2N + y)(2N + y + 2) + 1]\}. \end{aligned} \tag{6}$$

TABLE I. Excitation energies (normalized to the energy of the first excited state) and $B(E2)$ values [in units of $B(E2; 2_{1,1}^+ \to 0_{1,0}^+) = 1$] for the E(5) critical-point symmetry [1], for several $N = 5$ calculations, and for the experimental data of ^{134}Ba [13]. The finite-N calculations involve the exact diagonalization of the critical IBM Hamiltonian (H_{cri}) [Eq. (12)], τ-projected states for H_{cri} [Eqs. (6) and (9) with $y = 0.314$], the U(5) limit [ϵn_d], and the O(6) limit [$(A/4)(N - \sigma)(N + \sigma + 4) + B\tau(\tau + 3)$].

	E(5)	Exact $N = 5$	τ projection $N = 5$	U(5) $N = 5$	O(6) $N = 5$	^{134}Ba exp
$E(0_{1,0}^+)$	0	0	0	0	0	0
$E(2_{1,1}^+)$	1	1	1	1	1	1
$E(L_{1,2}^+)$	2.20	2.195	2.19	2	2.5	2.32
$E(L_{1,3}^+)$	3.59	3.55	3.535	3	4.5	3.66
$E(0_{2,0}^+)$	3.03	3.68	3.71	2	$1.5\frac{A}{B}$	3.57
$B(E2; 4_{1,2}^+ \to 2_{1,1}^+)$	1.68	1.38	1.35	1.6	1.27	1.56(18)
$B(E2; 6_{1,3}^+ \to 4_{1,2}^+)$	2.21	1.40	1.38	1.8	1.22	
$B(E2; 0_{2,0}^+ \to 2_{1,1}^+)$	0.86	0.51	0.43	1.6	0	0.42(12)

The $E_{\xi,\tau}$ are independent of L since H is an O(5) scalar. Their expressions involve the quantities $S_{k,\tau}^{(N)} = \langle \xi = 1; y, N, \tau | (s^\dagger)^k s^k | \xi = 1; y, N, \tau \rangle$ which are given by

$$S_{1,\tau}^{(N)} = (N - \tau + 1) \frac{G_{N-\tau}^{(\tau+1)}(y)}{G_{N-\tau+1}^{(\tau+1)}(y)}, \tag{7}$$

where $S_{2,\tau}^{(N)} = S_{1,\tau}^{(N)} S_{1,\tau}^{(N-1)}$ and $S_{3,\tau}^{(N)} = S_{1,\tau}^{(N)} S_{1,\tau}^{(N-1)} S_{1,\tau}^{(N-2)}$. Nondiagonal matrix elements of H between τ-projected states in different ξ bands, $H_{1,2;\tau} = \langle \xi = 2; y, N, \tau | H | \xi = 1; y, N, \tau \rangle$, can be evaluated as well:

$$H_{1,2;\tau} = 2\mathcal{N}_\beta [S_{2,\tau}^{(N)}]^{1/2} \{\epsilon y + \tfrac{1}{4} A(y-1)[(2N + y + 1) + 2(y-1) S_{1,\tau}^{(N-2)}]\}. \tag{8}$$

By techniques similar to that employed in the O(6) limit of the IBM [11], explicit expressions of quadrupole rates can be derived for transitions between the τ-projected states. For the relevant IBM quadrupole operator, $T(E2) = d^\dagger s + s^\dagger \tilde{d}$, these transitions are subject to the O(5) selection rule $\Delta\tau = \pm 1$, and, as explained in the caption of Fig. 1, it is sufficient to focus on the $B(E2)$ values of the type

$$\begin{aligned} B(E2; \xi = 1; \tau + 1, L = 2\tau + 2 \to \xi = 1, \tau, L = 2\tau) &= \frac{(\tau + 1)}{(2\tau + 5)(N - \tau + 1)} (S_{1,\tau}^{(N)})^2 \frac{G_{N-\tau+1}^{(\tau+1)}(y)}{G_{N-\tau}^{(\tau+2)}(y)} \\ &\quad \times \left[y + (N - \tau) \frac{G_{N-\tau-1}^{(\tau+2)}(y)}{G_{N-\tau}^{(\tau+1)}(y)} \right]^2, \end{aligned} \tag{9}$$

$$B(E2; \xi = 2, \tau, L = 2\tau \to \xi = 1, \tau + 1, L = 2\tau + 2) = \frac{(\tau + 1)(4\tau + 5)}{(4\tau + 1)(2\tau + 5)} 4\mathcal{N}_\beta^2 y^2 (y - 1)^2 (N - \tau) \frac{G_{N-\tau-1}^{(\tau+1)}(y)}{G_{N-\tau}^{(\tau+2)}(y)}.$$

The states in Eqs. (3) and (5) can be obtained by O(5) projection from the IBM intrinsic states for the ground band

$$\begin{aligned} |c; N\rangle &= (N!)^{-1/2} (b_c^\dagger)^N |0\rangle, \\ b_c^\dagger &= (1 + \beta^2)^{-1/2} \left[\beta \cos\gamma d_0^\dagger + \beta \sin\gamma \frac{1}{\sqrt{2}} (d_2^\dagger + d_{-2}^\dagger) + s^\dagger \right] \end{aligned} \tag{10}$$

and, respectively, for the β band

$$|\beta; N\rangle = \mathcal{N}_\beta P_y^\dagger |c; N - 2\rangle, \tag{11}$$

provided $y = \beta^2$. The expressions in Eqs. (3)–(9) depend on the, so far, unspecified parameter y. Normally, the equilibrium value of β, and hence y, is chosen as the global minimum of the intrinsic energy surface determined from the expectation value of H in the intrinsic state (10). This is a standard procedure for a Hamiltonian describing nuclei with rigid shapes, for which the global minimum is deep and well localized. However, near the critical point of the phase transition an alternative procedure is required.

The IBM Hamiltonian, $H_{\rm cri}$, at the critical point of the U(5)-O(6) phase transition corresponds [9] to a special choice of parameters in the Hamiltonian of Eq. (1)

$$H_{\rm cri} : \epsilon = (N - 1)A. \tag{12}$$

The intrinsic energy surface of $H_{\rm cri}$ has the form

$$E(\beta) = E_0 + AN(N - 1)\beta^4 (1 + \beta^2)^{-2}, \tag{13}$$

where $E_0 = \frac{1}{4} AN(N - 1)$ is a constant. The energy surface $E(\beta)$, shown in Fig. 2(a), has a flat behavior ($\sim \beta^4$) for small β, an inflection point at $\beta = 1$, and approaches a constant for large β. The global minimum at $\beta = 0$ is not well localized and $E(\beta)$ exhibits considerable instability in β, resembling a square-well potential for $0 \le \beta \le 1$. Under such circumstances fluctuations in β are large and play a significant role in the dynamics. Some of their effect can be taken into account by introducing into the intrinsic states of Eqs. (10) and (11) an effective β

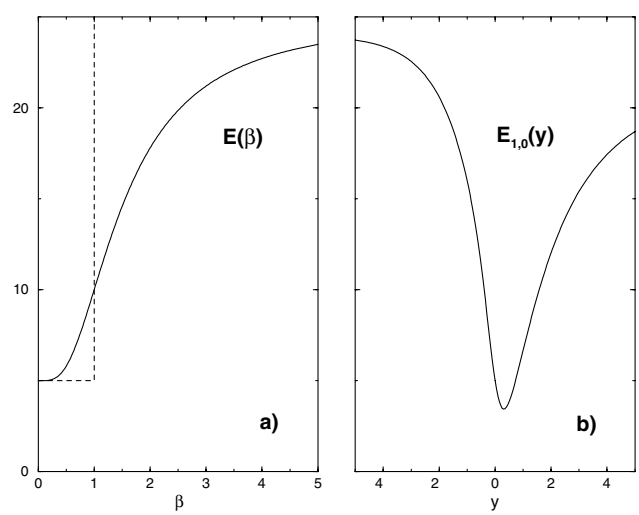

FIG. 2. Energy surfaces of the critical IBM Hamiltonian $H_{\rm cri}$ (12) with $N = 5$ and $A = 1$. (a) Intrinsic energy surface $E(\beta)$, Eq. (13) (solid line), and its approximation by a square-well potential (dashed line). (b) O(5) projected energy surface $E_{\xi=1,\tau=0}(y)$, Eq. (6). The global minimum is at $y = 0.314$.

TABLE II. U(5) decomposition (in %) of the $L^+_{\xi,\tau}$ states for $N = 5$. The calculated values are obtained from the τ-projected states, Eqs. (4) and (5) with $y = 0.314$. The exact values are obtained from numerical diagonalization of the critical IBM Hamiltonian $H_{\rm cri}$, Eq. (12).

	$0^+_{1,0}$		$2^+_{1,1}$		$L^+_{1,2}$		$L^+_{1,3}$		$0^+_{2,0}$	
n_d	Calc	Exact	Calc	Exact	Calc	Exact	Calc	Exact	Calc	Exact
0	83.2	83.4							15.8	16.4
1			92.2	90.2						
2	16.4	16.2			96.8	95.2			70.9	76.2
3			7.8	9.7			99.1	98.4		
4	0.4	0.4			3.2	4.8			13.3	7.4
5			0.0	0.1			0.9	1.6		

deformation. The effective deformation is expected to be in the range $0 < y = \beta^2 < 1$, in between the respective U(5) and O(6) values of β. This will enable a reproduction of E(5) characteristic signatures which are in between these limits (see Table I). In contrast to $E(\beta)$, we see from Fig. 2(b) that the O(5) projected energy surface $E_{\xi=1,\tau=0}(y)$ of $H_{\rm cri}$ [Eqs. (6) and (12) with $N = 5$] does have a stable minimum at a certain value of y, which we interpret as an effective β deformation. This procedure, based on variation after projection, is in the spirit of [14] in which it is shown that in finite boson systems, a γ-unstable O(6) state can be generated from a rigid triaxial intrinsic state with an effective γ deformation of 30°. In the present case the γ instability is treated exactly by means of O(5) symmetry, while the β instability is treated by means of an effective deformation. The appropriate value of y can be used to evaluate the band mixing, $\eta_\tau(y) = \frac{|H_{1,2;\tau}|}{E_{2,\tau} - E_{1,\tau}}$. A small value of η_τ will ensure that the τ-projected states of Eqs. (3) and (5) form a good representation of the actual eigenstates of $H_{\rm cri}$ and turn the expressions of Eqs. (6) and (9) into meaningful estimates for energies and quadrupole transition rates at the critical point.

To test the suggested procedure we compare in Table II the U(5) decomposition of exact eigenstates obtained from numerical diagonalization of $H_{\rm cri}$ for $N = 5$ with that calculated from the τ-projected states with $y = 0.314$ [the global minimum of $E_{1,0}(y)$]. As can be seen, the latter provides a good approximation to the exact eigenstates (the corresponding band mixing is $\eta_\tau = 0.12\%$, 3.53%, 4.14%, 3.05% for $\tau = 0, 1, 2, 3$). This agreement in the structure of wave functions is translated also into an agreement in energies and $B(E2)$ values as shown in Table I. The results of Tables I and II clearly demonstrate the ability of the suggested procedure to provide analytic and accurate estimates to the exact finite-N calculations of the critical IBM Hamiltonian, which in turn agree with the experimental data in ^{134}Ba and captures the essential features of the E(5) critical-point symmetry.

To summarize, in this work we have considered properties of a critical-point symmetry in a finite system. We have focused on the E(5) critical-point symmetry corresponding to flat-bottomed potentials as encountered in a second-order phase transition between spherical and deformed γ-unstable nuclei. We have shown that intrinsic states with an effective β deformation reproduce the dynamics of the underlying nonrigid shapes. The effective deformation can be determined from the global minimum of the energy surface after projection onto the appropriate symmetry. In the present case, states of fixed N and good O(5) symmetry projected from these intrinsic states provide good analytic estimates to the exact eigenstates, energies, and quadrupole transition rates at the critical point.

This work was supported in part by the Israel Science Foundation (A. L.) and in part by the U.S. Department of Energy under Contract No. W-7405-ENG-36 (J. N. G).

[1] F. Iachello, Phys. Rev. Lett. **85**, 3580 (2000).
[2] F. Iachello, Phys. Rev. Lett. **87**, 052502 (2001).
[3] R. F. Casten and N.V. Zamfir, Phys. Rev. Lett. **85**, 3584 (2000).
[4] J. M. Arias, Phys. Rev. C **63**, 034308 (2001).
[5] A. Frank, C. E. Alonso, and J. M. Arias, Phys. Rev. C **65**, 014301 (2002).
[6] N.V. Zamfir *et al.*, Phys. Rev. C **65**, 044325 (2002).
[7] Da-li Zhang and Yu-xin Liu, Phys. Rev. C **65**, 057301 (2002).
[8] F. Iachello and A. Arima, *The Interacting Boson Model* (Cambridge University Press, Cambridge, 1987).
[9] A. E. L. Dieperink, O. Scholten, and F. Iachello, Phys. Rev. Lett. **44**, 1747 (1980).
[10] J. N. Ginocchio and M.W. Kirson, Phys. Rev. Lett. **44**, 1744 (1980); J. N. Ginocchio and M.W. Kirson, Nucl. Phys. **A350**, 31 (1980).
[11] A. Arima and F. Iachello, Ann. Phys. (N.Y.) **123**, 468 (1979).
[12] M. A. Caprio, Phys. Rev. C **65**, 031304 (2002).
[13] Yu. V. Sergeenkov, Nucl. Data Sheets **71**, 557 (1994).
[14] T. Otsuka and M. Sugita, Phys. Rev. Lett. **59**, 1541 (1987).